Data acquisition system for a proton imaging apparatus

V.Sipala[a,b], M.Brianzi[c], M.Bruzzi[c,d], M.Bucciolini[c,e], G.Candiano[f], L.Capineri[g], G.A.P.Cirrone[f], C.Civinini[c], G.Cuttone[f], D.Lo Presti[a,b], L.Marrazzo[c,e], E.Mazzaglia[f], D.Menichelli[c,d], N.Randazzo[b], C.Talamonti[c,e], M.Tesi[d], S.Valentini[c,g].

[a] Dipartimento di Fisica, Università degli Studi di Catania, via S. Sofia 64, I-95123, Catania, Italy.
[b] INFN, sezione di Catania, via S. Sofia 64, I-95123, Catania, Italy.
[c] INFN, sezione di Firenze, via G. Sansone 1, I-50019 Sesto Fiorentino (FI), Italy.
[d] Dipartimento di Energetica, Università degli Studi di Firenze, via S. Marta 3, I-50139 Firenze, Italy.
[e] Dipartimento di Fisiopatologia Clinica, Università degli Studi di Firenze, v.le Morgagni 85, I-50134 Firenze,Italy.
[f] INFN, Laboratori Nazionali del Sud, via S. Sofia 62, I-95123, Catania, Italy.
[g] Dipartimento di Elettronica e Telecomunicazioni, Università degli Studi di Firenze, via S. Marta 3, I-50139 Firenze, Italy.

valeria.sipala@ct.infn.it

Abstract

New developments in the proton-therapy field for cancer treatments, leaded Italian physics researchers to realize a proton imaging apparatus consisting of a silicon microstrip tracker to reconstruct the proton trajectories and a calorimeter to measure their residual energy. For clinical requirements, the detectors used and the data acquisition system should be able to sustain about 1 MHz proton rate. The tracker read-out, using an ASICs developed by the collaboration, acquires the signals detector and sends data in parallel to an FPGA. The YAG:Ce calorimeter generates also the global trigger. The data acquisition system and the results obtained in the calibration phase are presented and discussed.

I. Introduction

The proton therapy is a good clinical treatment for cancer as it permits to obtain a dose distribution extremely conform to the target volume. In order to fully exploit the potential of proton dose release, the dose calculation should be performed with high accuracy. This issue requires the knowledge of proton stopping power inside the tissues. Up to now this information is deduced from X-Rays Computed Tomography, but the error related to this procedure is relevant. To overcome this problem, proton imaging can be used as a direct method for stopping power determination. Moreover, the same imaging system can be useful in the patient positioning verification.

The aim of the Italian project [1] is to develop a proton imaging system with density and spatial resolution less than 1% and 1 mm respectively, as clinical demands [2]. The apparatus presented reconstructs the map of the electron density by tracking the single proton through the traversed tissue and by measuring its residual energy. In fact, previous our studies [3]-[5] indicate that proton imaging based on tracking of individual protons traversing an object from many different directions and measuring their energy loss and scattering angle may yield accurate reconstructions of electron density maps with good density and spatial resolution, despite the fundamental limitation of Multiple Coulomb Scattering (MCS).

II. Proton Imaging Apparatus Design

The proton imaging apparatus developed by the Italian collaboration includes a tracker with four x-y planes based on position sensitive microstrip detectors to determine particle entry and exit point and direction. Each tracker plane consists of two modules with sensors and electronic read-out positioned at 90° to each other.

Downstream the tracker, a calorimeter is used for residual energy measurement. It consists of four YAG:Ce crystals optically separated and coupled in the same housing. Its read-out system acquires the information about the residual energy of the particle and generates the trigger signal and the system global event number in order to label each single proton.

The proton energy used in a proton imaging apparatus, must be 250-270MeV in order to cross the entire patient thickness[2]. Moreover, using the “single tracking technique”, to acquire an image in a fraction of a secondthe, the system should be able to sustain 1MHz proton beam.

III. Data Acquistion System

The Fig.1 shows the architecture of the data acquisition system. Before starting the data acquisition, all tracker modules must send a trigger enable signal to the trigger generator board. When the single particle traverses all tracker modules and it is stopped in the calorimeter, the global trigger signal and the global event number are generated and sent to all tracker modules and to the calorimeter acquisition board. Then, the tracker modules and the calorimeter board acquire data in parallel mode and move data in a buffer memory. Finally, by an Ethernet commercial module the data are transferred to a PC in order to reconstruct the most likely path. The data in all tracker modules and in the calorimeter are labelled by the global event number used to associate unambiguously the data to the corresponding single proton crossing.

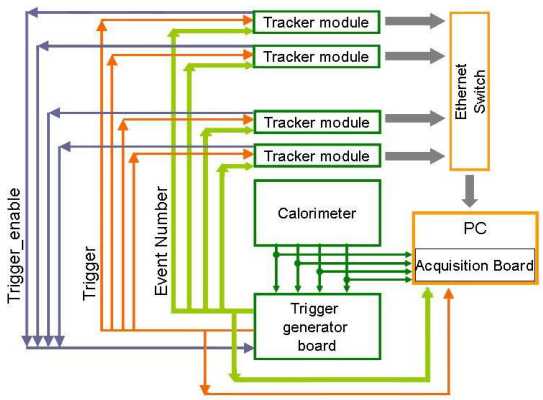

Figure 1: The architecture of the data acquisition system of the proton imaging apparatus that the Italian collaboration is realizing.

A. *Tracker read-out*

The tracker module includes a front-end board and a digital board. The detector is a 256-microstrip silicon detector, produced by Hamamatsu [6], with 200 µm of thickness and 200 µm of pitch. The active area is 53 x 53mm^2.

The silicon detector, positioned in the front-end board, is coupled with eight ASICs each serving 32 front-end channels. The integrated circuit, developed by the collaboration in CMOS AMS 0.35u technology, via a charge sensitive amplifier, a shaper and a comparator, converts the fast current signal from the microstrip crossed by the particle, in a digital pulse of 300-800ns width. The duration of the pulse depends on the amount of energy released by the proton and on the threshold value used. So, for fixed threshold value, by the Time Over Threshold (TOT) technique it is possible also to measure the charge released into the silicon detector.

In order to achieve 1MHz data acquisition rate, the outputs signals are sent in parallel mode to an FPGA located on the digital board which performs zero suppression and moves data to a buffer memory. An Ethernet commercial module is use both for data transfer to the central acquisition PC and to control the tracker module DAQ parameters.

B. *Calorimeter read-out*

The material chosen as calorimeter of proton imaging apparatus is a YAG:Ce scintillating crystals. In fact, thanks to the fast scintillating light decay constant (70ns), this crystal is able to sustain 1MHz proton rate. Moreover, the characteristic wavelength of maximum emission (550ns) permits to couple the crystal with a commercial photodiode which resolves the problem of sensitivity to the magnetic field in the gantry. The calorimeter area is 60 x 60 cm^2 to a depth of 10cm, fixed to stop proton until 200MeV.

The read-out system consists of four charge sensitive amplifiers and four shapers. The outputs are sampled by a commercial acquisition Board at 14bit and 50MHz (UltraFast 2-4000 [7]). The number of samples needed to reconstruct the pulse is acquired. By data interpolation the amplitude of the signal is obtained, which is proportional to the proton residual energy.

In the readout system an hybrid charge sensitive amplifier, with a low decay constant, will be used. As explained in [8] a low-noise non-inverting amplifier is inserted in a conventional charge-amplifier configuration (see Fig. 2). So the discharge current is increased due to the increased voltage drop across the feedback resistor R_F. The decay time constant seen at the preamplifier's output is thus reduced. In particular, the charge-to-voltage sensitivity is increased by a factor equal to the gain of non-inverting amplifier and the decay constant decreases by the same factor. This configuration permits to obtain a high acquisition rate and a low noise.

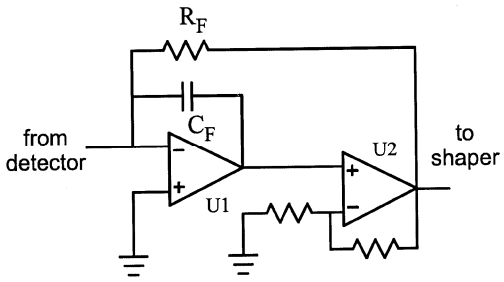

Figure 2: Schematic of the hybrid charge sensitive preamplifier that will be used in the calorimeter readout in order to achieve a high acquisition rate.

C. *Trigger system*

The trigger signal is generated using the calorimeter outputs: each calorimeter output is compared with a fixed threshold voltage to produce a digital pulse. Four digital pulses are summed so that, when one of four crystals is crossed by proton, a trigger signal is produced.

The trigger signal forces the acquisition board to store into its local memory the samples of the calorimeter outputs and every FPGA to read its input latches and to store the data in the onboard RAM memory using zero-suppression.

Moreover, the trigger signal increases the counting of the global event number that is attached to all the data generated by the tracker modules and by the calorimeter.

The trigger board has been realized using commercial devices.

IV. Results

The proton imaging apparatus is in advanced status of realization. In a previous work [9] the first results obtained with only the front-end board have been shown.

At present, a x-y plane of the tracker (front-end board coupled with the digital board) is ready to be tested with proton beam. Each tracker module must be calibrated before to be test with proton beam. The results of a single tracker module calibration are presented in this section. The test with a beta source permit to conclude that the module is fully efficiency for released energy lower than expected with proton imaging application.

The YAG:Ce calorimeter has been characterized with different proton beam energies: the preliminary results are discussed.

A. *Calibration phase of tracker module*

During the calibration phase, all 256-microstrips of the detector have been characterized using a test pulse connected to the front-end chip input by integrated test capacitance. In the last front-end board prototype, each chip, containing 32 front-end channels, has an adjustable threshold voltage value to allow for a better chip optimization. The strip outputs are acquired by the FPGA, moved to the buffer memory, transferred to the PC and analyzed off-line.

The Fig. 3 shows the calibration curves with the pulse duration as function of the input charge. With this data and using the TOT technique, it is possible to estimate the charge released by the particle inside the detector.

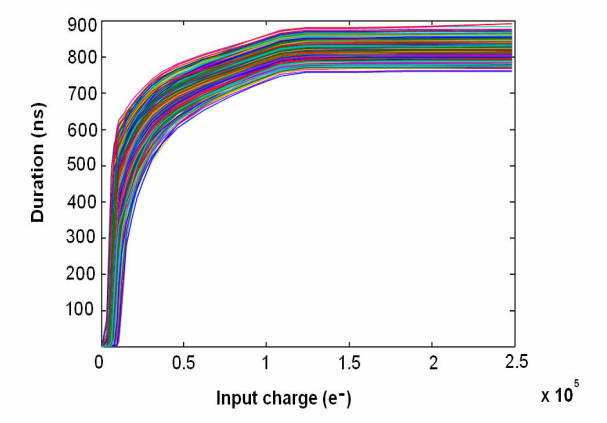

Figure 3: Calibration curves of all detector channels. The pulse duration vs. input charge has been plotted.

The other test have been performed in order to estimate the threshold voltage dispersion and the minimum input charge that it is possible to reveal with our tracker module.

In the Fig. 4, for a fixed input charge value (Q=5MIP), the efficiency of all channels is shown as function of the threshold voltage value. The tracker plane is full efficient even at a threshold voltage which is 240mV above the minimum the baseline. The threshold dispersion within the full module can be estimated to be of the order of 70mV.

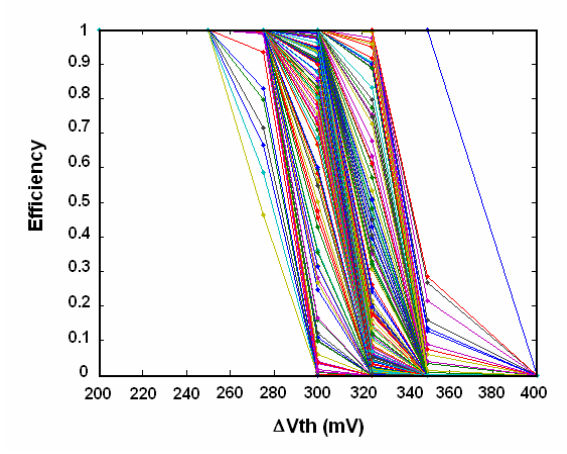

Figure 4: Plot of the efficiency for all channels vs. the threshold voltage value: the module is fully efficient up to ΔVth<240mV.

Fixing the threshold voltage values at minimum level over the noise, the efficiency curves have been plotted for different input charge values in order to estimate the minimum input charge to reveal. As shown in Fig. 5, the system is fully efficient when a charge equivalent to the most probable released by a MIP is injected. A MIP in 200µm of silicon creates about 15000 electrons.

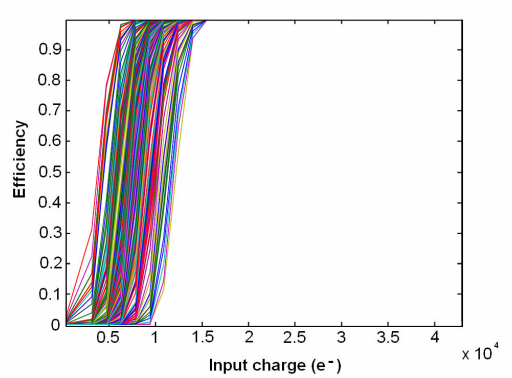

Figure 5: Plot of the efficiency for all channels vs. the input charge value: the module is fully efficient for injected charge greater than 15000e- (=1MIP).

B. *Acquisition with beta source*

The single tracker module has been tested using a beta source (^{90}Sr). A low noise scintillator has been placed downstream the detector in order to generate the trigger signal. A total of about 100000 events have been acquired at a maximum rate of about 20kHz. Using the pulse duration and the calibration data, the released charge in each single channel has been calculated.

Moreover, a study of the time dependences between the trigger signal and the pulse delay has been performed. The distribution of strip pulse start respect to the trigger is shown in Fig. 6. Most of the counts are located before the trigger signal. The trigger signal is more fast than the strip pulses, so, it is necessary to acquire in pre-triggering mode. The FPGA provides continuous signal sampling but sends to buffer memory only the samples in the time window centred on the trigger signal.

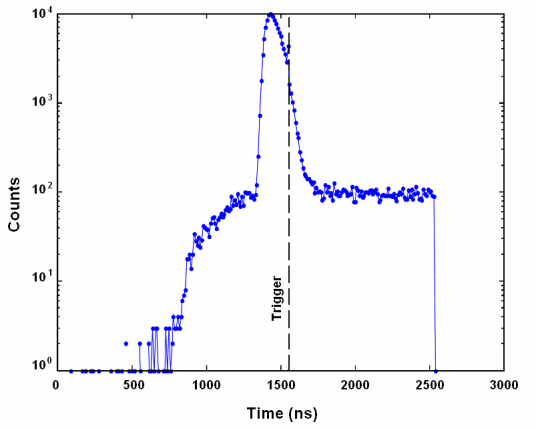

Figure 6: Time distribution of a single tracker channel obtained with beta source. The histogram maximum is located before the trigger signal.

For higher released energy, the pulse duration increases and the delay decreases. This effect is clearly visible in Fig. 7 where the counts map of the delay signal respect to trigger start is plotted against pulse duration values. The maximum of the counts (red in the figure) shows a delay decreasing when pulse duration increases.

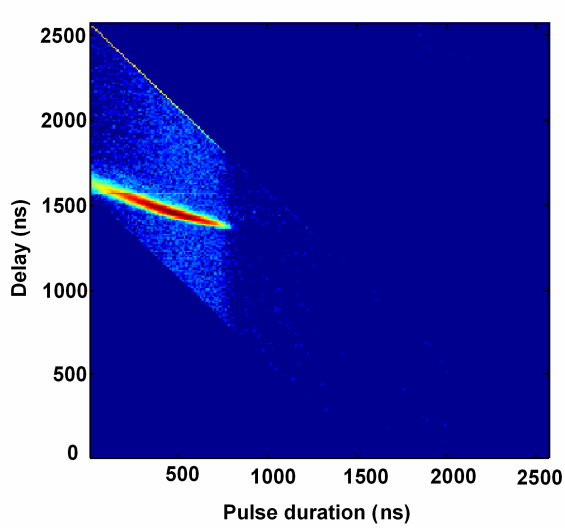

Figure 7: Counts map of the strip pulse delay respect to the pulse duration. The delay decrease as the pulse duration increase.

C. *Characterization of the calorimeter*

The YAG:Ce calorimeter has been characterized at Laboratori Nazionali del Sud and at Loma Linda University Medical Center with different proton beam energies. Using a standard acquisition system, the crystal responses at different proton energies has been observed. As example, in Fig. 8 the charge spectrum obtained with a single crystal and 100MeV proton beam is shown. The system has a good resolution equal to 2,7 %.

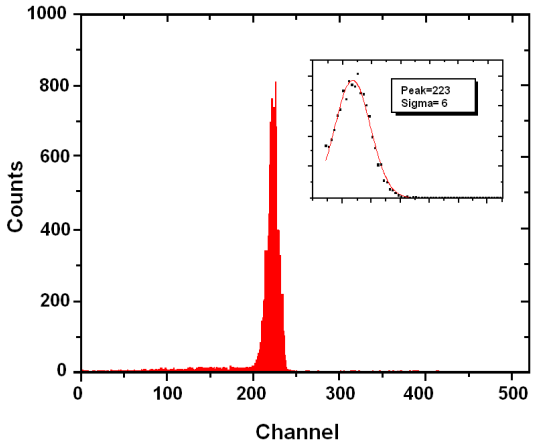

Figure 8: Charge spectrum obtained with 100MeV proton beam and a single crystal of the calorimeter: the resolution is equal to 2.7%.

In order to test the linearity of the single crystal the charge spectrum for three different energy values have been acquired. The Fig. 9 shows the peak position in the charge spectrum as function of the proton energy: in an energy range comprised between 35-200MeV the response of the crystal is linear with 1.15 % error.

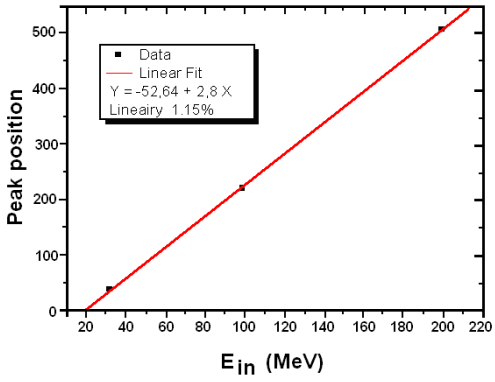

Figure 9: Peak position in the charge spectrum vs. the proton beam energy. In 35-200MeV energy range the linearity is equal to 1.15%.

Each crystal has been characterized and shows a good resolution at different energies and a good linearity in 35-200MeV energy range.

V. Conclusions

A proton imaging apparatus is being built by the Italian collaboration. The goal is to realized a system able to obtain an imagine by reconstruction of the most likely path of the single particle, knowing its entry and exit position and direction and its residual energy. This technique permits to resolve the problem introduced of the multiple coulomb scattering of the proton in the matter. For clinical requirements, the detectors used and the data acquisition system should be able to sustain about 1 MHz proton rate.

The detectors has been chosen, the architecture of the data acquisition system has been fixed, a ASICs containing 32 front-end channels has been developed and the complete data acquisition system is in advanced status of realization.

Each module of the tracker must be calibrated: the results obtained with a single module have been presented in this paper.

The YAG:Ce crystal calorimeter was completely characterized using a front-end electronics with commercial parts. A new electronic front-end with higher acquisition rate has been developed and will be used in the next test.

A x-y plane of the tracker is ready to be tested with protons and coupled with YAG:Ce calorimeter. The next step will be test the system at Laboratori Nazionali del Sud with 62MeV proton beam.

VI. References

[1] G.A.P. Cirrone et al. – Nucl. Instr. and Meth. A 576 (2007) 194–197

[2]R. Shulte, et al., IEEE Trans. Nucl. Sci. Vol.51, N.3 (2004).

[3] G. A. Pablo Cirrone et al. , IEEE Trans. Nucl. Sci, Vol. 54, N. 5, (2007)

[4] M. Bruzzi, et al. IEEE Trans. Nucl. Sci. Vol.54, N.1 (2007).
[5] C. Talamonti, et al., Nucl. Instr. and Meth. A (2009), doi:10.1016/j.nima.2009.08.040
[6] http://www.hamamatsu.com
[7] http://www.strategic-test.com
[8] R. Bassini, C. Boiano and A. Pallia, IEEE Trans. Nucl. Sci. Vol. 49 N.5 (2002)
[9] V. Sipala et al., Nucl. Instr. and Meth. A (2009), doi:10.1016/j.nima.2009.08.029.